JOURNAL OF VIROLOGY, Nov. 1999, p. 9011–9020 Vol. 73, No. 11
0022-538X/99/$04.00+0

Structure-Based Mutagenesis of the Human Immunodeficiency Virus Type 1 DNA Attachment Site: Effects on Integration and cDNA Synthesis

HEIDI E. V. BROWN, HONGMIN CHEN, AND ALAN ENGELMAN*

Department of Cancer Immunology and AIDS, Dana-Farber Cancer Institute and the Department of Pathology, Harvard Medical School, Boston, Massachusetts 02115

Received 26 May 1999/Accepted 30 July 1999

Sequences at the ends of linear retroviral cDNA important for integration define the viral DNA attachment (*att*) site. Whereas determinants of human immunodeficiency virus type 1 (HIV-1) integrase important for replication in T lymphocytes have been extensively characterized, regions of the *att* site important for viral spread have not been thoroughly examined. Previous transposon-mediated footprinting of preintegration complexes isolated from infected cells revealed enhanced regions of bacteriophage Mu insertion near the ends of HIV-1 cDNA, in the regions of the *att* sites. Here, we identified the subterminal cDNA sequences cleaved during in vitro footprinting and used this structure-based information together with results of previous work to construct and characterize 24 *att* site mutant viruses. We found that although subterminal cDNA sequences contributed to HIV-1 replication, the identities of these bases were not critical for integration. In contrast, the phylogenetically conserved CA dinucleotides located at the ends of HIV-1 contributed significantly to virus replication and integration. Mutants containing one intact CA end displayed delays in peak virus growth compared to the wild type. In contrast, double mutant viruses lacking both CAs were replication defective. The A of the CA appeared to be the most critical determinant of integration, because two different U5 mutant viruses containing the substitution of TG for CA partially reverted by changing the G back to A. We also identified a U5 deletion mutant in which the CA played a crucial role in reverse transcription.

The primary product of reverse transcription in retrovirus-infected cells is linear double-stranded DNA containing a copy of the viral long terminal repeat (LTR) at each end. Efficient viral replication requires the integration of this cDNA into a host cell chromosome. Retroviral integration is mediated by the viral integrase protein acting on the ends of the linear cDNA substrate. The viral DNA attachment (*att*) site is defined as those end sequences important for integration. The *att* site is comprised of U3 sequences at the outer edge of the 5′ LTR and U5 sequences at the tip of the 3′ LTR.

Integrase is a polynucleotidyl transferase. In an initial endonucleolytic step, integrase processes each 3′ end of the DNA adjacent to CA dinucleotides that are conserved among all retroviral *att* sites. Integrase then attaches the recessed CA ends to the 5′ phosphates of a double-stranded staggered cut in a chromosomal DNA target site. The resulting gapped structure is repaired, presumably by host cell enzymes, resulting in the integrated provirus 5′ TG. . .CA 3′ flanked by the sequence duplication of the double-stranded cut. For a recent review of retrovirus integration, see reference 5.

In infected cells, integration takes place in the context of large nucleoprotein structures called preintegration complexes (PICs). PICs isolated from infected cells can integrate their endogenous cDNA into an added target DNA in vitro (6, 10, 13, 20). Using bacteriophage Mu-mediated PCR (MM-PCR) footprinting, we recently described the native protein-DNA structure of PICs isolated from cells infected with wild-type human immunodeficiency virus type 1 (HIV-1). Evidence for strong protein binding was detected only in the end regions of HIV-1 cDNA (7), and the footprinting pattern at each end was bipartite. First, bound proteins caused hot spots for Mu insertion within the terminal 5 to 25 bp, in the regions of the U3 and U5 *att* sites. Second, the subterminal regions from approximately 25 to 250 bp were protected from Mu transposition (7). Similar footprinting and enhancement patterns were detected in PICs isolated from cells infected with Moloney murine leukemia virus (Mo-MuLV) (35), suggesting that this end-specific nucleoprotein complex may be a common structural element of retroviruses. This protein-DNA structure has been termed the "intasome" to distinguish it as a component of the greater PIC (7, 35).

In this study, we identified the DNA end sequences in the HIV-1 intasome that are preferentially cleaved during MM-PCR footprinting. The role of these and other nearby bases in the function of the HIV-1 *att* site was addressed by analyzing the replication capacities of 24 mutant viruses. We found that the CA conserved at the very ends of HIV-1 is the most significant determinant of virus viability, since both small and large changes made upstream of these bases did not profoundly affect virus growth unless the CA was concurrently altered. The A of the CA appeared to be most important, because two different U5 mutant viruses containing the substitution of TG for CA partially reverted by replacing the G with A. We also found that the CA was a critical determinant of cDNA synthesis in the context of a U5 deletion mutation.

MATERIALS AND METHODS

Construction of *att* site mutant plasmids. Plasmids pNL4-3 (1), p83-10, and p83-2 (15) were previously described. A unique *Xma*I site was introduced at the cellular-LTR DNA boundary in the pNL4-3 5′-half genome plasmid p83-2, generating p83-2/XmaI. The *Aat*II-*Sph*I fragment from p83-2/XmaI was swapped for the corresponding pNL4-3 fragment, generating an infectious molecular clone of pNL4-3 (pNL43/XmaI) lacking approximately 1.1 kb of 5′ flanking human DNA. All *att* site changes were introduced into pNL43/XmaI.

* Corresponding author. Mailing address: Department of Cancer Immunology and AIDS, Dana-Farber Cancer Institute, 44 Binney St., Boston, MA 02115. Phone: (617) 632-4361. Fax: (617) 632-3113. E-mail: alan_engelman@dfci.harvard.edu.

U5 and U3 changes were built into *Aat*II-*Sph*I and *Bam*HI-*Bsp*EI restriction fragments, respectively, by overlapping PCR with Pfu DNA polymerase (Stratagene, La Jolla, Calif.). Mutant *Aat*II-*Sph*I fragments were ligated to *Aat*II-*Sph*I-digested pNL43/XmaI DNA. Mutant *Bam*HI-*Bsp*EI fragments were first shuttled into the 3′-half genome plasmid p83-10. An exception was U3 mutant 3; it contained a novel *Bam*HI restriction site, and was therefore shuttled as an *Hpa*I-*Bsp*EI fragment. *Nhe*I-*Pml*I fragments containing the U3 changes were then incorporated into pNL43/XmaI. The presence of the mutations, as well as the absence of off-site changes, was confirmed by dideoxy sequencing. U3/U5 double mutants were built by incorporating mutant *Aat*II-*Sph*I fragments into the appropriately digested U3 mutant pNL43/XmaI plasmids.

Cells and viruses. 293T cells (26) were grown in Dulbecco's modified Eagle medium containing 10% fetal calf serum (FCS). Jurkat (37), CEM-12D7 (29), C8166 (31), SupT1 (32), and MOLT-IIIB (13) T-cell lines were grown in RPMI 1640 medium containing 10% FCS.

293T cells seeded at 5.8×10^4 cells/cm^2 in a 10-cm-diameter dish 24 h prior to transfection were transfected with 20 μg of plasmid DNA by using calcium phosphate (33). Cell supernatants were tested for Mg^{2+}-dependent ^{32}P-reverse transcriptase (RT) activity as described previously (11), and equal RT counts per minute of wild-type and mutant viruses were used to infect CD4$^+$ T-cell lines. Unless otherwise noted, Jurkat cells (2×10^6) infected with 10^6 RT cpm (approximately 10^4 infectious particles [29]) for 18 h in 0.5 ml were washed and plated in 5 ml of RPMI containing 10% FCS. Cells were split every 2 to 3 days, and aliquots were saved for ^{32}P-RT assays. Each mutant virus was analyzed in a minimum of two independent experiments.

Analysis of viral DNA synthesis. Viral DNA synthesis was detected by either PCR or Southern blotting. For PCR, CEM-12D7 cells (5×10^6) were infected with 10^6 RT cpm for 1.5 h in 0.5 ml. Cells were washed, plated in 5 ml of RPMI containing 10% FCS, and lysed 18 h postinfection as described previously (11). The two-LTR-containing circular form of HIV-1 DNA was detected by nested PCR as follows. Cell lysate (10 μl) was reacted in 50 μl of buffer containing 10 mM Tris-HCl (pH 8.3), 50 mM KCl, 1.5 mM $MgCl_2$, 0.001% gelatin, 0.2 mM each deoxynucleoside triphosphate (dNTP), 0.5 μM each AE452 (5′ CACCAT CCAAAGGTCAGTGGATATC 3′; NL4-3 minus-strand bases 136 to 112) and AE609 (5′ TTGAGTGCTTCAAGTAGTGTGTGCC 3′; plus-strand positions 9615 to 9639), and 2 U of Ampli*Taq* DNA polymerase (Perkin-Elmer Corp., Foster City, Calif.). Reaction mixtures were heated at 95°C for 2 min, followed by 20 cycles of denaturation (95°C for 15 s), annealing (58°C for 1 min), and extension (72°C for 45 s). Reactions were then extended for 7 min at 72°C. Portions (2 μl) were transferred into a second PCR round (25 μl) containing the same buffer as the first round, 0.5 μM each nested primers AE347 (5′ GTCAG TGGATATCTGATCCCTG 3′; minus-strand bases 124 to 103) and AE346 (5′ GAGATCCCTCAGACCCTTTTAG 3′; plus-strand bases 9666 to 9687), 2×10^5 cpm of ^{32}P-end-labeled AE347, and 1 U of Ampli*Taq* polymerase. Reactions were cycled as described for the first round. Second-round portions (4 μl) were electrophoresed through 5% polyacrylamide gels, the gels were dried, and DNA was detected by autoradiography.

For Southern blotting, C8166 cells (1.5×10^7 in 10 ml) were infected with equal RT counts per minute of wild-type or mutant HIV-1 (7×10^7 to 9×10^7 total RT cpm in repeated experiments) for 8 h. Cells were lysed, and DNA was recovered, electrophoresed through agarose, and analyzed by Southern blotting with a riboprobe that detects minus-strand DNA as previously described (7). Levels of cDNA synthesis were quantified with a PhosphorImager (Molecular Dynamics, Sunnyvale, Calif.).

Isolation of HIV-1 PICs. PICs were isolated from acutely infected cells by using one of two different tissue culture infection systems. Infection with the human T-cell leukemia virus 3B (HTLV-3B) strain of HIV-1 was initiated by mixing chronically infected MOLT-IIIB cells with uninfected SupT1 cells (7). In the other system, C8166 cells were infected with the NL4-3 strain produced by transfection (7). PICs were isolated from infected cells and purified for MM-PCR footprinting as previously described (7).

MM-PCR footprinting and generation of DNA sequencing ladders. MM-PCR was performed as previously described (7). In this footprinting technique, the frequency and distribution of Mu transposition into a target DNA are detected by using two rounds of PCR (7, 35). In this study, native and deproteinized HIV-1 PICs were the targets of DNA footprinting. HIV-1 primers for generating sequencing ladders for mapping the positions of Mu transposition were designed as follows. One of the MM-PCR primers is Mu specific. The 5′ end of this Mu primer lies 44 nucleotides upstream from the Mu DNA end that cut the footprinting target (7). To account for this distance, the 5′ ends of HIV-1 sequencing primers were designed 44 bases upstream of the 5′ ends of second-round HIV-1 MM-PCR primers. This technique allows mapping the positions of Mu transposition into a footprinting target to within 1 or 2 nucleotides.

DNA sequencing ladders were generated with the Circumvent Thermal Cycle DNA Sequencing kit (New England BioLabs, Inc., Beverly, Mass.). Plasmid substrates for sequencing reactions contained either the 5′ or 3′ LTR. Figure 1 presents the results for the HTLV-3B strain of HIV-1. To generate an appropriate 5′ LTR-containing plasmid, pSVC21, which contains the HXBc2 full-length molecular clone of HTLV-3B (28), was digested with *Eco*RI and *Xho*I, and the 6.95-kb *Eco*RI fragment containing the 5′ LTR was isolated and self-ligated. Plasmid pSVC21/3′-LTR was generated by digesting pSVC21 with *Eco*RI and *Sph*I, isolating the 5.96-kb *Eco*RI fragment, and ligating it with *Eco*RI-digested pSP73 (Promega Corp., Madison, Wis.) vector DNA.

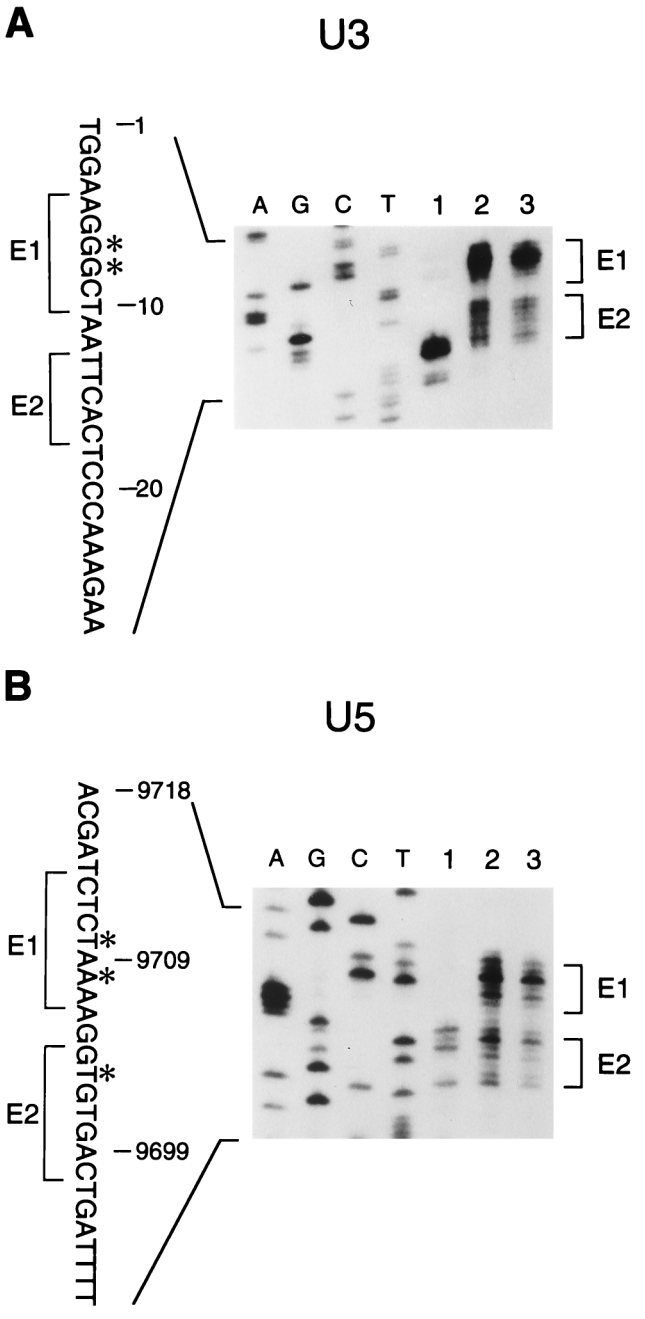

FIG. 1. HIV-1 sequences in native PICs cleaved during MM-PCR footprinting. (A) The U3 end of HIV-1. Footprinted deproteinized complexes diluted 1:2 (lane 1) were electrophoresed alongside 1:6 (lane 2) and 1:10 (lane 3) dilutions of native samples. Bases cut in native PICs are indicated to the right of the gel and alongside the DNA sequence to the left (E1 and E2). Most frequently cut bases are marked with asterisks. (B) The U5 end. The samples in lanes 1 to 3 were as described for panel A. The results for the HTLV-3B strain of HIV-1 are shown; the HXBc2 molecular clone of HTLV-3B (28) terminates at nucleotide 9718. The same bases of the NL4-3 strain of HIV-1 were cut by Mu. Because of the polarity of Mu transposition, only the termini of the unjoined HIV-1 strands (plus for U3, minus for U5) can be analyzed by MM-PCR. For simplicity, the positions of Mu insertion are shown on the plus strand in panel B.

The U3 and U5 HIV-1 second-round MM-PCR primers were AE452 and AE609, respectively; the sequence and positions of these primers in the NL4-3 genome were noted above. The U3 sequencing ladder (Fig. 1A) was generated with primer AE453 (5′ TGGCTTCTTCTAACTTCTCTGGCTC 3′; HXBc2 mi-

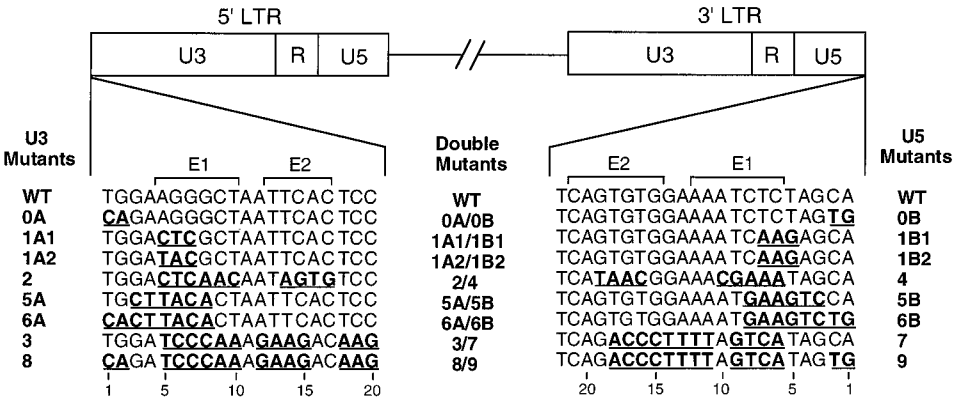

FIG. 2. HIV-1 *att* site mutants. Shown beneath the genetic map of proviral DNA is the plus-strand sequence. Bases introduced by mutagenesis are underlined in boldface. Upstream sequences that replaced the deleted bases in mutants 3, 7, 8, and 9 are shown. Nucleotides are numbered based on their positions with respect to the proviral termini. Mutations were introduced into plasmid DNA in the 5′ copy of U5 and the 3′ copy of U3. Following DNA transfection and viral infection, the mutated *att* sequences were duplicated by reverse transcription such that they also reside in the indicated end regions of proviral DNA. E1 and E2, the transpositional enhanced regions identified in Fig. 1. WT, wild type.

nus-strand bases 180 to 156) and pSVC21/5′-LTR; the U5 ladder (Fig. 1B) was generated with AE322 (5′ GGCTAACTAGGGAACCCACTG 3′; HXBc2 plus-strand bases 9580 to 9600) and pSVC21/3′-LTR. The U5 sequencing ladder for mapping Mu transposition into NL4-3 PICs was generated by using primer AE322 and plasmid p83-10. The NL4-3 U3 ladder was generated by using AE506 (5′ TTGCCTCCTCTACTTGC 3′; minus-strand bases 180 to 164) and p83-2/XmaI.

Detection of virion RNA. Virion RNA was detected in pelleted virus by using an RNase protection assay essentially as previously described (8). In brief, equal RT counts per minute from supernatants (8.5 ml) of cells transfected with either wild-type or *att* mutant plasmid DNA were pelleted through sucrose and lysed in 0.4 ml of 10 mM Tris-HCl (pH 7.5)–150 mM NaCl–5 mM EDTA–0.5% (wt/vol) sodium dodecyl sulfate. Following extraction with phenol-chloroform, RNA was recovered by precipitation with ethanol.

Equal amounts of wild-type and mutant viral lysates were analyzed with a commercially available RNase protection kit (Ambion, Inc., Austin, Tex.) with the minus-sense HXBc2-derived MB riboprobe spanning nucleotides 307 to 707 (8). This procedure yields a radiolabeled 3′ genomic U3R-containing RNA fragment of 244 nucleotides (8).

Cloning and sequencing of U5 revertant mutant viruses. Titers of mutant 0B, 6B, and 9 viruses harvested from infected Jurkat cells were determined for ^{32}P-RT content, and equal RT counts per minute of wild-type, mutant, and revertant viruses were passed onto fresh Jurkat cells. At the height of these second-round infections, revertant virus-infected cells were lysed by Hirt extraction as described previously (14). For analysis of the U5 regions of the viruses, DNA (10 to 25 μl) in the Hirt supernatant was PCR amplified with plus-sense primer AE606 (5′ GCTGCATCCGGAGTACTTCAAGAAC 3′; NL4-3 positions 9377 to 9401) and minus-sense AE597 (5′ GGCCCTGCATGCACTGGA TGC 3′; 1434 to 1454) with Pfu DNA polymerase. The resulting fragments were either sequenced directly, or cut with *Bsp*EI and *Sph*I and ligated to *Bsp*EI-*Sph*I-digested p83-2/XmaI DNA. For analysis of integrase sequences, 25 μl of Hirt supernatant was amplified by using plus-sense primer AE244 (5′ AAAGAACC GGTACATGGAGTGTATTATGAC 3′; 3480 to 3509) and minus-sense AE245 (5′ TTCCTCCATTCTATGGAGACTCCCTGACCCAAATG 3′; 5312 to 5278). The resulting DNA products were sequenced directly.

RESULTS

HIV-1 intasome sequences preferentially cleaved during MM-PCR footprinting. In MM-PCR footprinting, protein-DNA complexes are reacted in vitro with the Mu transpososome DNA cleavage reagent (35). A distinguishing characteristic of footprinted Mo-MuLV and HIV-1 PICs is that hot spots for Mu insertion exist near the very ends of the preintegrative cDNAs (7, 35). In order to map the HIV-1 sequences preferentially cut during MM-PCR footprinting, both native and deproteinized footprinted samples were analyzed by denaturing polyacrylamide gel electrophoresis alongside DNA sequencing ladders (Fig. 1).

The results of this analysis revealed that the U3 and U5 ends of native HIV-1 each contain two closely linked regions of transpositional enhancements. The U3 bases targeted most often were at positions 5 to 10 and 13 to 17 (Fig. 1A). For U5, positions 6 to 12 and 15 to 21 from the terminus were preferentially cleaved (Fig. 1B). In order to test whether these bases might have particular significance for viral replication, several *att* site mutant viruses incorporating changes in and around the enhanced regions were constructed.

Mutagenesis strategy. Twenty-four U3, U5, and U3/U5 *att* site mutant viruses were designed based on the revealed enhanced regions, as well as results of prior work (Fig. 2). One parameter we considered when targeting U5 is its proposed role in initiating reverse transcription (2, 4, 24). In the RNA genome, U5 *att* abuts the primer binding site (PBS), where the cellular tRNA that primes reverse transcription binds. Different regions of HIV-1 U5 *att* have been implicated in intramolecular RNA-RNA interactions, as well as intermolecular interactions with the $tRNA_3^{Lys}$ primer of reverse transcription. For example, the stretch of four A's at positions 10 to 13 in U5 (numbering defined in Fig. 2) interacts with the anticodon loop of $tRNA_3^{Lys}$ (18). Also, 5′ AUCUCUAG 3′ at positions 10 to 3 interacts with 5′ CUAGAGAU 3′ located upstream of the *att* site at positions 40 to 47 from the U5 terminus (17). We incorporated changes into this upstream region for a subset of mutants that targeted U5 *att* site positions 3 to 10.

HIV-1 mutants 3 and 7 targeted the U3 and U5 enhanced regions, respectively, by deletion. In mutant 3, bases 5 to 17 were removed. In mutant 7, positions 6 to 19 from the U5 terminus were deleted (Fig. 2). We did not include upstream changes in mutant 7 to compensate for possible perturbations in RNA secondary structure. Mutants 2 and 4 targeted the U3 and U5 enhanced regions, respectively, by base substitution. While mutant 2 targeted both U3 regions, mutant 4 was designed to change as much of U5 as possible without grossly disturbing the stretch of A's proposed to interact with $tRNA_3^{Lys}$ (Fig. 2). Positions 44 to 40 from the mutant 4 terminus were also altered to compensate for the changes at positions 6 to 10.

In addition to targeting the subterminal sequences revealed by MM-PCR footprinting, base substitution was used to test the roles of the sequences at the viral DNA termini. Mutants 0A and 0B tested the significance of the terminal CA dinucleotides that are conserved in all retroviral *att* sites (Fig. 2). Mutants 5A and 5B targeted the six bases directly abutting the conserved CAs at the U3 and U5 ends, respectively (Fig. 2). Positions 42 to 47 in mutant 5B were also changed, to mirror

the changes at positions 3 to 8. Additional mutants were designed to test the significance of the conserved CAs in the context of other internal changes. Mutant 8 combined the changes in U3 mutants 3 and 0A, and mutant 9 was a combination of U5 mutants 7 and 0B (Fig. 2). Similarly, mutant 6A combined the changes in mutants 5A and 0A, and mutant 6B combined the changes in 5B and 0B (Fig. 2).

Positions 5 to 7 from each terminus have been shown to be important for simian immunodeficiency virus (SIV) integration in infected cells (9). Mutants 1A1, 1A2, 1B1, and 1B2 targeted these sequences in HIV-1 (Fig. 2). Mutants 1A2, 1B1, and 1B2 contained the same base changes as those previously studied in SIV (9). Whereas compensatory changes were incorporated into mutant 1B1 at U5 positions 43 to 45, these upstream bases were left unchanged in mutant 1B2.

Virus replication. Virus stocks were generated by transfecting 293T cells with plasmids containing either wild-type or *att* site mutant HIV-1. Transfection of cells bypasses early steps in the HIV-1 life cycle, such as reverse transcription and integration, that may be disrupted by *att* site mutations. Cells transfected with each of the mutant plasmid DNAs yielded wild-type levels of RT activity in cell supernatants, suggesting that none of the *att* site mutations interfered with late steps in the HIV-1 life cycle, such as particle assembly and release from cells. Equal amounts of each virus in cell-free supernatants were then used to infect $CD4^+$ Jurkat T cells. Infected cultures were monitored for production of progeny virus for up to 60 days.

(i) Mutants containing changes internal to the CAs maintain their ability to replicate. Jurkat cells infected with wild-type HIV-1 supported peak replication 5 to 6 days postinfection (Fig. 3). The six different *att* mutant viruses containing changes at positions 5 to 7 from the HIV-1 termini replicated similarly to the wild type (Fig. 3B and C). Thus, these *att* site positions do not play a critical role in HIV-1 replication under these conditions. Also, the 3-bp mismatch at U5 positions 5 to 7 and 43 to 45 in the potential RNA stem of mutant 1B2 does not significantly impair HIV-1 replication.

Mutant viruses containing more drastic changes of subterminal *att* sequences also maintained their capacity to replicate. Mutants 5A and 5B, which contained changes at U3 and U5 positions 3 to 8, respectively, grew similarly to the wild type. In repeated experiments, the 5A/5B double mutant replicated with a 2-day delay compared to the wild type (Fig. 3E). Mutants 2 and 4, which contained changes in the U3 and U5 enhanced regions, respectively, also grew similarly to the wild type (Fig. 3D). The 2/4 double mutant grew with a 2-day delay compared to the wild type in repeated experiments. Mutant 7, which lacked U5 positions 6 to 19, also grew similarly to the wild type. Jurkat cells infected with its U3 counterpart, mutant 3, showed an initial 2-day delay in the appearance of RT counts per minute compared to wild-type-infected cells (Fig. 3G). In repeated experiments, cells infected with mutant 3 supported peak virus growth either the same day as the wild type (Fig. 3G) or delayed 2 days (data not shown). The combined 3/7 double mutant replicated with a 2- to 4-day delay compared to the wild type in repeated experiments.

(ii) Changes at both CA termini yield replication-defective viruses. Cells infected with mutant 0A, which contained the substitution of TG for the conserved CA at the U3 end, supported peak virus replication delayed 2 days compared to wild-type-infected cells (Fig. 3A). The U5 mutant 0B replicated with a 4-day delay compared to the wild type. Cells infected with the 0A/0B double mutant did not support detectable virus growth during a 60-day observation period.

Whereas U3 mutant 6A grew with an 8-day delay compared to the wild type, cells infected with the 6B U5 variant supported mutant growth delayed 13 to 18 days compared to the wild type (Fig. 3F; data not shown). Similarly to the 0A/0B double mutant, cells infected with 6A/6B failed to support detectable HIV-1 replication over a prolonged observation period.

Whereas mutant 8 in repeated experiments replicated with an 8-day delay compared to the wild type, mutant 9 replicated with a 10- to 30-day delay (Fig. 3H; data not shown). Cells infected with the 8/9 double mutant failed to support detectable mutant viral growth over the 2-month observation period. Table 1 summarizes the replication phenotypes of the *att* site mutant viruses.

TABLE 1. Summary of *att* site mutant phenotypes

Mutant	Replication[a]	cDNA synthesis[b]	RNA content[c]	Primary defect[d]
0A	++	+++	ND[e]	Int
0B	++	+++	ND	Int
0A/0B	−	+++	ND	Int
1A1	+++	ND	ND	NA[f]
1B1	+++	ND	ND	NA
1A1/1B1	+++	ND	ND	NA
1A2	+++	ND	ND	NA
1B2	+++	+++	ND	NA
1A2/1B2	+++	+++	ND	NA
2	+++	ND	ND	NA
4	+++	ND	ND	NA
2/4	++	+++	ND	Int
5A	+++	ND	ND	NA
5B	+++	ND	ND	NA
5A/5B	++	+++	ND	Int
6A	+	+++	ND	Int
6B	+	+++	ND	Int
6A/6B	−	+++	ND	Int
3	+++	+++	ND	NA
7	+++	+++	+++	NA
3/7	++	++	+++	Int + RT
8	+	++	+++	Int + RT
9	+	+/−	+++	RT
8/9	−	+	+++	Int + RT

[a] +++, replication peak detected the same day as that of the wild type; ++, replication delayed 2 to 4 days compared to that of the wild type; +, replication delayed 6 to 30 days compared to that of the wild type; −, replication not detected over a 60-day observation period.

[b] +++, 50 to 120% of the wild type level; ++, 25 to 50% of the wild-type level; +, 10 to 25% of the wild-type level; +/−, <10% of the wild-type level.

[c] +++, RNA content indistinguishable from that of the wild type.

[d] Replication-delayed or -defective mutants were ascribed a primary defect based on the results of Fig. 3 to 6. Int, primary defect at the integration step; RT, reverse transcription defect; Int + RT, mutant likely suffers both reverse transcription and integration defects.

[e] ND, not determined.

[f] NA, not applicable.

Certain *att* mutations dramatically affect cDNA synthesis. The results of the previous experiments revealed that our set of *att* site mutant viruses displayed a variety of replication phenotypes. Although replication-defective *att* site mutants might be expected to be blocked at the integration step in infected cells, U5 mutants can also be defective for reverse transcription (2, 24) or RNA packaging (see below). Thus, cDNA synthesis after infection was analyzed for each *att* site mutant virus that displayed a delay in replication compared to wild-type HIV-1.

DNA synthesis was monitored by using either PCR or Southern blotting. Preliminary experiments using nested PCR to detect the two-LTR-containing circular form of HIV-1 DNA revealed that many of the replication-delayed *att* site

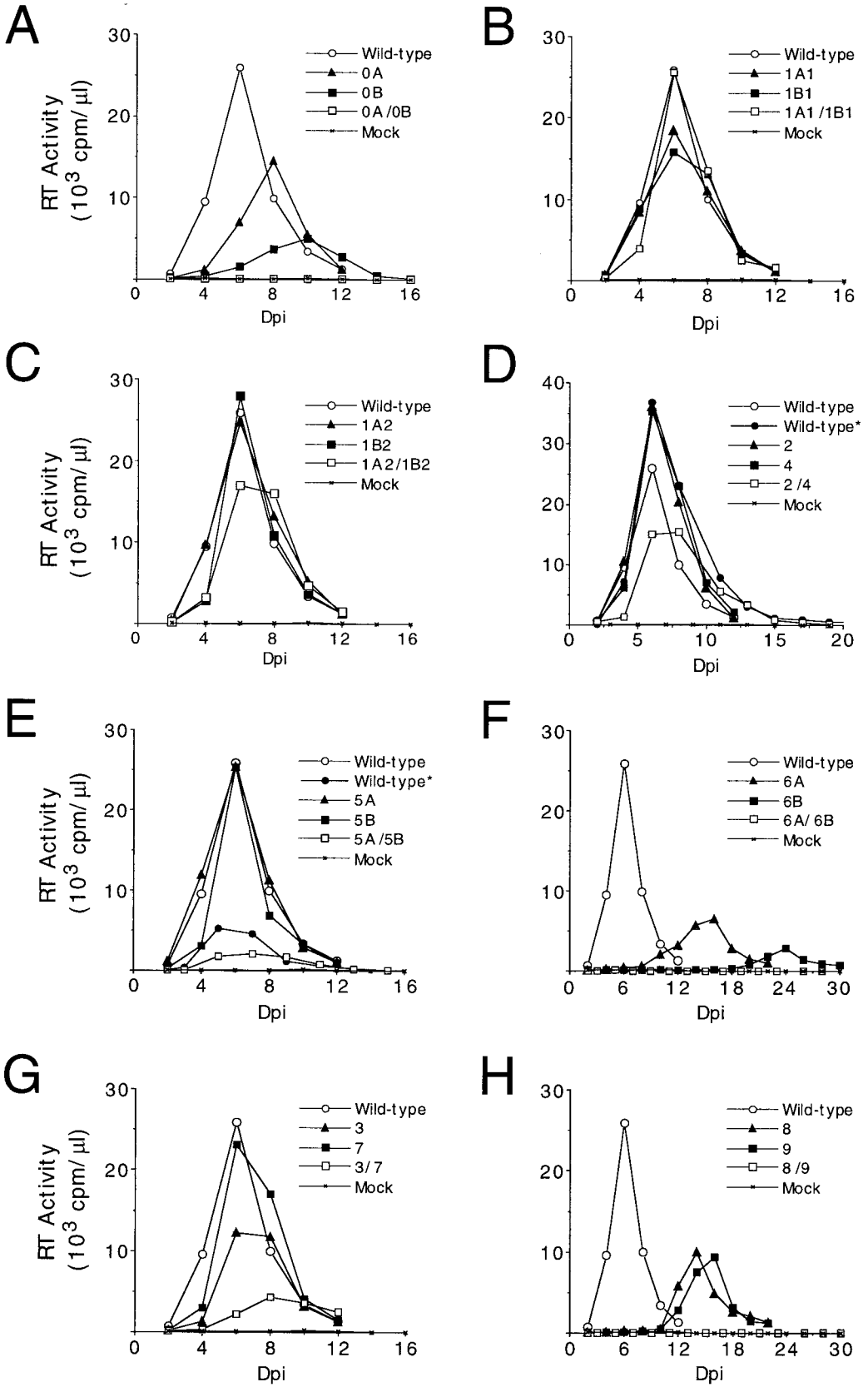

FIG. 3. Replication kinetics of wild-type and *att* site mutant HIV-1 in Jurkat cells. Cells infected with the indicated viruses were monitored for production of RT activity at the indicated time points. Wild-type* and mutant 2/4 in panel D were analyzed in a separate experiment from the wild type and mutants 2 and 4. Similarly, wild-type* and mutant 5A/5B in panel E were from a separate experiment. Although the wild type reproducibly reached its peak growth 5 to 6 days postinfection, the yield of wild-type particles varied as much as sixfold in repeated experiments (panel E [see also Fig. 6B and C]). Dpi, days postinfection.

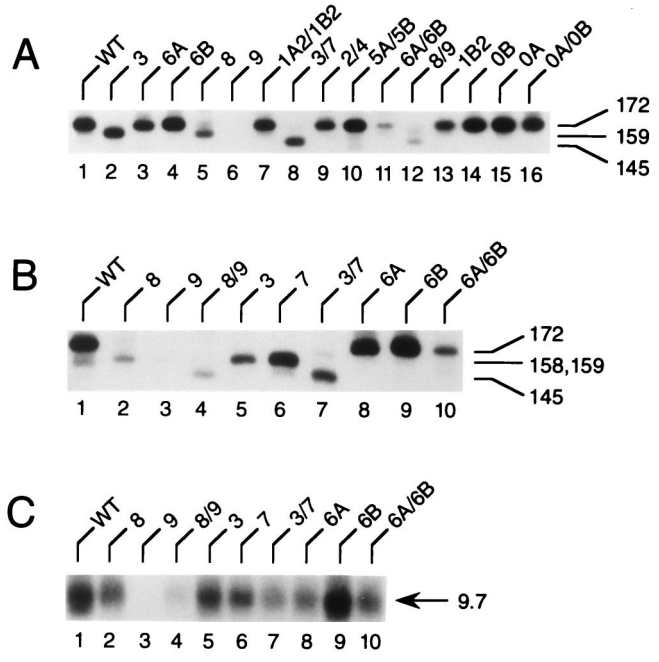

FIG. 4. Wild-type and *att* site mutant cDNA synthesis in infected cells. (A and B) Cells infected with either the wild-type (WT) or the indicated *att* site mutant were analyzed for two-LTR circle content by PCR. The predicted sizes of product DNA for full-length and single and double deletion mutants are indicated on the right in base pairs. (C) Cells infected with the indicated viruses were analyzed for cDNA content by Southern blotting. The size of the full-length minus strand is indicated on the right in kilobase pairs.

mutant viruses supported a level of cDNA synthesis similar to that of the wild type (Fig. 4A and Table 1). Since cells infected with the 0A/0B double mutant virus contained the wild-type level of HIV-1 DNA (Fig. 4A, lanes 1 and 16), we conclude that 0A/0B is replication defective due to a block in integration (Table 1). On the other hand, mutants 8, 9, 8/9, and 6A/6B synthesized noticeably lower levels of the two-LTR circle than did the wild type (Fig. 4A, lanes 1, 5, 6, 11, and 12). Mutant 7, which differed from mutant 9 by 2 bp (Fig. 2) and replicated similarly to the wild type (Fig. 3G), was therefore included in a subsequent experiment. The results of this experiment confirmed that cells infected with mutants 8, 9, and 8/9 contained reduced levels of two-LTR circular DNA compared to wild-type-infected cells (Fig. 4B, lanes 1 to 4). In contrast, cells infected with mutant 7 contained a level of HIV-1 DNA similar to that in wild-type-infected cells (lanes 1 and 6). Thus, the CA→TG substitution in concert with the 14-bp deletion present in mutant 7 significantly impaired the ability of mutant 9 to synthesize cDNA in infected cells (Fig. 4B, compare lanes 3 and 6).

Whereas the results of Fig. 4A suggested that cells infected with mutant 6A/6B supported a level of cDNA synthesis similar to that detected for mutant 8/9, the results presented in Fig. 4B implied that mutant 6A/6B might not be quite this defective for reverse transcription. In order to discount possible errors in quantitation that can be associated with PCR, we quantified cDNA synthesis in the absence of DNA amplification by using Southern blotting. The results of this experiment for the most part confirmed those of PCR: cells infected with mutant 9 contained approximately 20-fold less cDNA than wild-type-infected cells (Fig. 4C, compare lane 3 to lane 1). Whereas cells infected with mutant 8/9 contained about fivefold less cDNA than wild-type-infected cells (Fig. 4C, compare lane 4 to lane 1), cells infected with 3/7 contained about threefold less cDNA (lane 7). In contrast, cells infected with mutants 8, 3, 7, 6A, 6B, and 6A/6B contained at most a twofold reduction in the level of cDNA compared to wild-type-infected cells in repeated experiments (Table 1). Mutant 6B-infected cells reproducibly contained more HIV-1 cDNA than cells infected with the wild type (Fig. 4C, lanes 1 and 9). This apparent increase in the level of HIV-1 cDNA compared to that in the wild type was also detected by PCR (Fig. 4B, lanes 1 and 9).

***att* site mutants and incorporation of virion RNA.** In addition to its roles in integration and reverse transcription, U5 sequences also influence the packaging of genomic RNA into assembling virus particles (22, 24). Since cells infected with mutant 9 contained dramatically reduced levels of HIV-1 cDNA, wild-type and mutant particles were pelleted and analyzed for viral RNA content by RNase protection.

The results of this experiment revealed that virus particles derived from mutants 8, 9, 8/9, 7, and 3/7 contained a similar level of genomic RNA as did wild-type particles (Fig. 5). It therefore appears that *att* site mutant 9 is primarily defective for reverse transcription in infected cells (Table 1).

Cloning and sequencing of revertant viruses: identification of sequences important for efficient integration and reverse transcription. Whereas a majority of our *att* site mutant viruses replicated similarly to the wild type, a subset of viruses grew with significant replication delays (Fig. 3F and H). Two alternatives for delayed growth can be considered. Either the mutants are simply slow replicators, or the viruses may need to acquire compensatory secondary mutations to replicate above the limit of detection in our in vitro assays. In an attempt to distinguish between these two possibilities, mutant viruses were harvested from infected Jurkat cells at their peaks of replication, their titers were determined for ^{32}P-RT content, and they were passed onto fresh Jurkat cells. Inherently slow growers would be expected to display the same replication phenotype in both initial and second-round infections. In contrast, viruses that acquired compensatory mutations would be expected to replicate more similarly to the wild type in second-round infections.

At a reduced multiplicity of infection compared to those used in Fig. 3, mutant 0B reached its peak replication 14 days after the wild type (Fig. 6A). However, virus harvested from

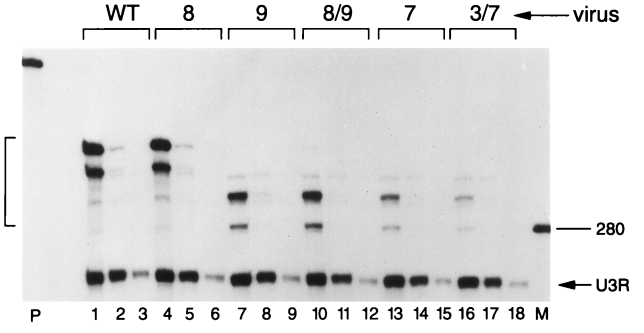

FIG. 5. RNA content of wild-type and *att* site mutant virions. Purified virion RNA was analyzed by RNase protection, and reaction products were analyzed by 5% sequencing gel. Each set of three lanes contained RNA corresponding to approximately 4.3×10^6, 1.1×10^6, and 0.3×10^6 RT cpm of either wild-type (WT) or the indicated mutant virus. The size of the 244-nucleotide U3R protected RNA fragment is marked to the right of the gel. One-tenth of the level of full-length probe MB used in the reactions in lanes 1 to 18 was loaded in lane P. Lane M contained a 280-base riboprobe marker (8). The bracket to the left of the gel indicates MB sequences protected by the 5′ LTR regions of plasmid DNAs left over from transfection.

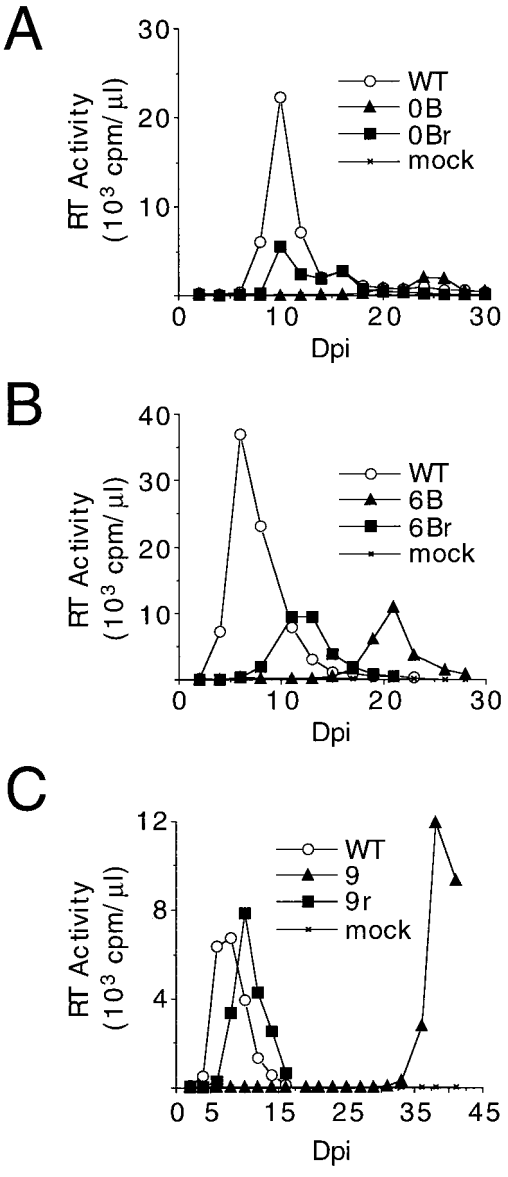

FIG. 6. Replication kinetics of U5 revertant viruses. (A) Jurkat cells (5×10^6) were infected with 0.5×10^6 RT cpm of the indicated viruses for 1.5 h, washed, and plated in 5 ml of medium. Aliquots of cell supernatants were saved at the indicated time points. (B and C) Cells infected with the indicated *att* site mutant and revertant viruses. WT, wild type. Other labeling is as described in the legend to Fig. 3.

these 0B-infected cells and passed onto fresh Jurkat cells reached its replication peak the same day as wild-type virus (Fig. 6A). The second-round-infected cells were lysed by Hirt extraction, and the U5 region of HIV-1 DNA was amplified by PCR. The resulting DNA fragment was cloned, and 12 separate plasmid DNA isolates were sequenced across their U5-containing regions. The results of this analysis revealed that the CA→TG substitution at the U5 end of mutant 0B partially reverted back to TA in 11 of the 12 clones; AA was found in place of TG in one of the clones.

Virus from 6B-infected Jurkat cells was similarly analyzed. Whereas cells infected with mutant 6B supported a peak in replication delayed 16 days compared to the wild type (Fig. 6B), cells infected with the 6Br revertant virus supported peak replication delayed only 6 days. Cells actively growing 6Br were lysed, and the PCR-amplified U5-containing DNA fragment was sequenced directly. This result revealed that the 5′ GAA GTCTG 3′ sequence at the end of the 6B mutant partially reverted to 5′ GAAGTCTA 3′. To investigate whether the improved growth of the revertant viruses involved changes in integrase, PCR fragments containing the 3′ end of the *pol* genes of 0Br and 6Br were sequenced. The integrase regions of these viruses maintained their wild-type sequences. Since both the starting 0B and 6B mutants synthesized wild-type levels of HIV-1 cDNA (Fig. 4), we conclude that the A of the conserved CA is a critical determinant for the effective integration of the 0Br and 6Br viruses in infected cells.

Virus harvested from infected Jurkat cells at the height of mutant 9 replication also showed a significant increase in replication kinetics upon reinfection (Fig. 6C). These second-round-infected cells were lysed and subjected to PCR. Sequencing of the 9r revertant virus across U5 revealed that the original mutant end 5′ GTCATAGTG 3′ reverted to 5′ GTC ATAGCA 3′, which was identical in sequence to mutant 7 (Fig. 2). The integrase region of the 9r revertant virus also did not reveal any detectable sequence differences from wild-type HIV-1.

DISCUSSION

Integration of retrovirus cDNA into an infected cell chromosome is required for efficient virus replication. The key viral players in integration are the *trans*-acting integrase protein and the *cis*-acting viral DNA *att* site. Whereas elements of HIV-1 integrase important for viral replication in T lymphocytes have been extensively studied, determinants of the *att* site important for efficient viral spread have not been well characterized.

Transpositional enhancements in native PICs and HIV-1 replication. In this study, we constructed and analyzed a set of 24 *att* site mutant HIV-1 viruses for their abilities to support spreading viral infections in $CD4^+$ Jurkat T lymphocytes. Our mutagenesis strategy was in part directed by identifying the viral end sequences cut during the in vitro MM-PCR footprinting of native PICs (Fig. 1 and 2). We found that mutating these sequences, which encompassed approximately positions 5 to 20 from each cDNA terminus, did not profoundly affect the replication capacity of HIV-1. Indeed, even the 2/4 and 3/7 U3/U5 double mutant viruses replicated with only slight delays compared to the wild type (Fig. 3D and G). These results are consistent with a recent analysis of the Mo-MuLV *att* site. Similar to the E2 regions in HIV-1, positions 17 to 22 from the Mo-MuLV U3 terminus were cleaved during in vitro MM-PCR footprinting (36). Deletion of positions 10 to 31 changed the sequence of the enhanced region without affecting either Mo-MuLV replication (25) or the positions of the transpositional enhancements with respect to distance from the cDNA end (36). Based on this observation, we speculate that mutants 2/4 and 3/7 possess E1 and E2 regions at the same positions relative to the U3 and U5 termini as does wild-type HIV-1, but that the sequences that define E1 and E2 for these mutants differ from those of the wild type (Fig. 2).

The basis for the transpositional enhancements detected during MM-PCR footprinting is at present unknown. Bacteriophage Mu and retroviruses both integrate DNA by using one-step transesterification chemistry (23), and recombinant HIV-1 integrase preferentially inserts synthetic *att* site DNA substrates into regions of known target DNA distortion (27). Thus, protein binding in native PICs may distort end regions of retroviral cDNA, and in doing so create hot spots for Mu insertion. Alternatively, viral end-specific protein factors may physically interact with the Mu transpososome.

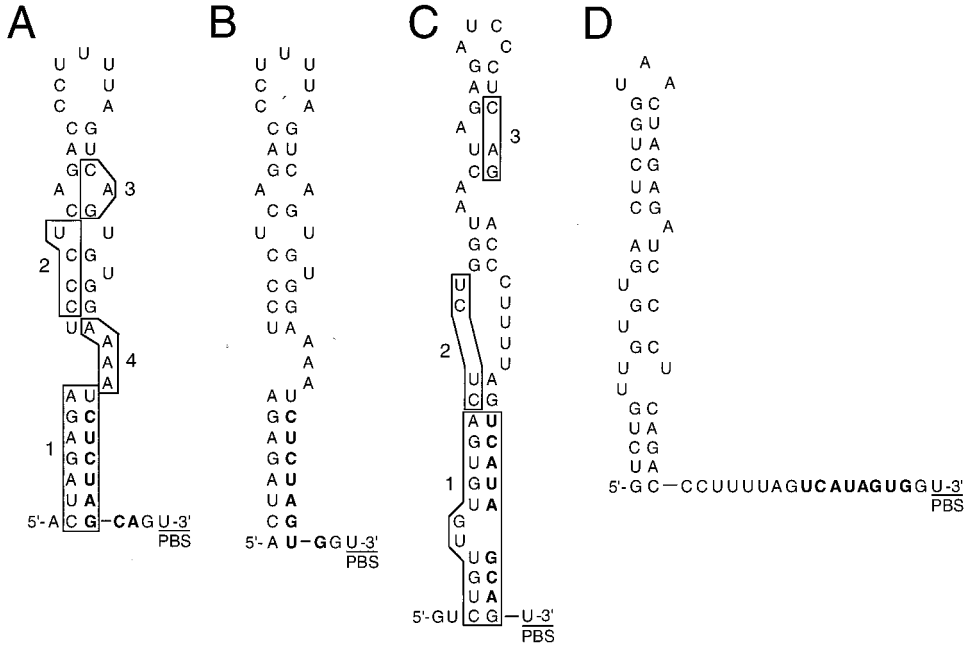

FIG. 7. Predicted secondary structures of wild-type and *att* mutant RNA. (A) Nucleotides 587 to 636 of wild-type RNA. In the presence of $tRNA_3^{Lys}$, the sequences in boxes 2, 3, and 4 interact with the primer (17). Box 1 indicates an intramolecular interaction detected in the presence of $tRNA_3^{Lys}$ (17). The 5′ end of the PBS is marked; *att* sequences (U5 positions 1 to 8) are in boldface. (B) The folded mutant 0B structure; other labeling is as in panel A. (C) Nucleotides 567 to 622 of mutant 7 RNA; note that the conserved CA is engaged near the base of the stem. Box 1 highlights secondary structure analogous to box 1 in panel A. Boxes 2 and 3 indicate sequences that could potentially interact with $tRNA_3^{Lys}$. The stretch of four A's (box 4 in panel A) thought to be important for initiating reverse transcription are deleted in mutant 7; others have noted that deletion of these bases does not significantly affect HIV-1 cDNA synthesis in infected cells (21). (D) The minimum-energy structure (−53.9 kcal/mol) of mutant 9 RNA analogous to the mutant 7 fold in panel C.

***att* site sequences important for HIV-1 replication.** Although deletion mutants 3 and 7 grew similarly to the wild type (Fig. 3G), addition of the CA→TG terminal substitution to either of these single-end mutant viruses profoundly impacted the ability of HIV-1 to replicate (Fig. 3H). Thus, the increased replication delay suffered by mutant 8 compared to mutant 0A highlights the contribution of U3 subterminal *att* site positions to HIV-1 replication. The result is that the subterminal *att* site change must be combined with the CA→TG change to reveal the contribution of the internal DNA sequence to HIV-1 replication under our assay conditions. The same holds true for subterminal *att* site positions 3 to 8. In this case, the 5A and 5B viruses replicated like the wild type (Fig. 3E), yet the 6A and 6B viruses suffered greatly pronounced replication delays compared to the 0A and 0B viruses, respectively (compare Fig. 3F and A). We conclude that *att* site positions 3 to 8 play an important role, but that the phylogenetically conserved CA dinucleotides are the most significant *att* site determinants of HIV-1 replication. Similar results were observed by analyzing the abilities of U3, U5, and U3/U5 *att* mutant viruses to express the gene for firefly luciferase in single-round infection assays (21).

Our finding that the 0Br and 6Br revertant viruses each contained the back substitution of TA for TG in U5 highlights the importance of the terminal adenine residue for HIV-1 integration in infected cells. Similarly to 0Br, a Mo-MuLV mutant carrying thymidine in place of cytosine at position 2 in U5 replicated with only a slight delay compared to the wild type (30). The importance of the terminal adenine residue in U5 *att* site integration has also been observed in in vitro integration assays (12).

At present the relationship between the relatively small size of retrovirus *att* sites and the relatively large size of cDNA protected from transposition during MM-PCR footprinting is unclear. One model predicts that only those cDNAs whose 3′ ends have been processed by integrase display the intasome structure as detected by MM-PCR footprinting (7). This is in part based on results from other DNA recombination systems. In Mu transposition, for example, the stability of the nucleoprotein complex increases with each successive chemical step down the recombination pathway (23). Thus, protein factors associated with the end regions of retrovirus cDNA might bind the DNA more tightly after 3′ processing than before this step. Future experiments are planned to test this hypothesis.

The U5 *att* site and HIV-1 reverse transcription. Although U5 mutant 7 synthesized nearly wild-type levels of HIV-1 cDNA in infected cells, mutant 9, which was identical to mutant 7 save for the added CA→TG substitution, was defective for cDNA synthesis (Fig. 4 and 5). Since U5 mutants 0B and 6B also contained the CA→TG change and synthesized wild-type levels of cDNA (Fig. 4), the mutant 9 defect must result from a collaboration between the 14-base deletion in mutant 7 and the CA→TG substitution. This interpretation was supported by analyzing the 9r revertant, since this virus was identical in sequence to mutant 7. We speculate that levels of reverse transcription sufficient for the spread of mutant 7 in our tissue culture infections require both the A and C at U5 positions 1 and 2, respectively.

The double mutant 8/9, although defective for reverse transcription, reproducibly synthesized more cDNA than the sole U5 mutant (Fig. 4). Although the basis for this is unknown, we speculate that U3 and U5 *att* may interact during reverse transcription of the 8/9 mutant virus.

At which step in the reverse transcription process might mutant 9 be defective? Mutant 9 synthesized about 20-fold less minus-strand DNA than the wild type (Fig. 4C). Minus-strand

synthesis is mostly complete partway through the reverse transcription process (34). Thus, mutant 9 is apparently defective relatively early in reverse transcription. There is precedence for the involvement of U5 *att* in initiating reverse transcription (2, 4, 24). Various RNA structures important for HIV-1 initiation have been proposed based on genetic, biochemical, and computer modeling data (3, 4, 16, 17, 19). We likewise analyzed *att* site mutant RNA by using the folding algorithm M-fold (38). Based on our genetic data, we postulated that the conserved CA in mutant 7 would be engaged in a secondary RNA structure, and this structure would be disrupted by the added CA→TG change in mutant 9. In contrast, the CA→TG substitution alone, which did not effect cDNA synthesis of mutant 0B, would not perturb wild-type RNA secondary structure.

Folding nucleotides 458 to 677 (numbering based on proviral DNA) of wild-type NL4-3 encompassing most of R, all of U5, the PBS, and 26 downstream bases yielded a minimum energy of −59.0 kcal/mol at 37°C (Fig. 7A). Mutant 0B yielded a very similar structure of minimum energy −60.9 kcal/mol (Fig. 7B). Mutant 7 yielded a minimum-energy folding of −54.8 kcal/mol. This optimized fold, however, did not show the conserved CA engaged in a secondary RNA interaction (data not shown). Mutant 7 folded into a second structure of very similar minimum energy (−54.5 kcal/mol) that did show the CA engaged (Fig. 7C). Mutant 9 also folded into alternate structures; the one of lowest free energy (−54.8 kcal/mol) was identical to the optimized mutant 7 structure, save for the CA→TG change (data not shown). In contrast, the CA→TG change dramatically altered the structure of the alternate mutant 7 fold (Fig. 7D). Future experiments are planned to further define the step at which mutant 9 is blocked for minus-strand synthesis in infected cells.

ACKNOWLEDGMENTS

We thank H. Göttlinger for plasmids and valuable discussion and D. Harris and N. Nakajima for critical review of the manuscript. Plasmids p83-2 and p83-10 were obtained by R. Desrosiers through the NIH AIDS Research and Reference Reagent Program.

This work was supported by NIH grant AI39394, by funds from the G. Harold and Lelia Y. Mathers Foundation, and by a gift from the Friends 10.

REFERENCES

1. **Adachi, A., H. E. Gendelman, S. Koenig, T. Folks, R. Willey, A. Rabson, and M. A. Martin.** 1986. Production of acquired immunodeficiency syndrome-associated retrovirus in human and nonhuman cells transfected with an infectious molecular clone. J. Virol. **59:**284–291.
2. **Aiyar, A., D. Cobrinik, Z. Ge, H.-J. Kung, and J. Leis.** 1992. Interaction between retroviral U5 RNA and the TψC loop of the $tRNA^{Trp}$ primer is required for efficient initiation of reverse transcription. J. Virol. **66:**2464–2472.
3. **Arts, E. J., M. Gosh, P. S. Jacques, B. Ehresmann, and S. F. J. Le Grice.** 1996. Restoration of tRNALys3-primed (−)-strand DNA synthesis to an HIV-1 reverse transcriptase mutant with extended tRNAs. J. Biol. Chem. **271:**9054–9061.
4. **Baudin, F., R. Marquet, C. Isel, J.-L. Darlix, B. Ehresmann, and C. Ehresmann.** 1993. Functional sites in the 5′ region of human immunodeficiency virus type 1 RNA form defined structural domains. J. Mol. Biol. **229:**382–397.
5. **Brown, P. O.** 1997. Integration, p. 161–203. *In* J. M. Coffin, S. H. Hughes, and H. E. Varmus (ed.), Retroviruses. Cold Spring Harbor Laboratory, Cold Spring Harbor, N.Y.
6. **Brown, P. O., B. Bowerman, H. E. Varmus, and J. M. Bishop.** 1987. Correct integration of retroviral DNA in vitro. Cell **49:**347–356.
7. **Chen, H., S.-Q. Wei, and A. Engelman.** 1999. Multiple integrase functions are required to form the native structure of the human immunodeficiency virus type 1 intasome. J. Biol. Chem. **274:**17358–17364.
8. **Dorfman, T., J. Luban, S. P. Goff, W. A. Haseltine, and H. G. Göttlinger.** 1993. Mapping of functionally important residues of a cysteine-histidine box in the human immunodeficiency virus type 1 nucleocapsid protein. J. Virol. **67:**6159–6169.
9. **Du, Z., P. O. Ilyinskii, K. Lally, R. C. Desrosiers, and A. Engelman.** 1997. A mutation in integrase can compensate for mutations in the simian immunodeficiency virus *att* site. J. Virol. **71:**8124–8132.
10. **Ellison, V., H. Abrams, T. Roe, J. Lifson, and P. Brown.** 1990. Human immunodeficiency virus integration in a cell-free system. J. Virol. **64:**2711–2715.
11. **Engelman, A., G. Englund, J. M. Orenstein, M. A. Martin, and R. Craigie.** 1995. Multiple effects of mutations in human immunodeficiency virus type 1 integrase on viral replication. J. Virol. **69:**2729–2736.
12. **Esposito, D., and R. Craigie.** 1998. Sequence specificity of viral end DNA binding by HIV-1 integrase reveals critical regions for protein-DNA interaction. EMBO J. **17:**5832–5843.
13. **Farnet, C. M., and W. A. Haseltine.** 1990. Integration of human immunodeficiency virus type 1 DNA in vitro. Proc. Natl. Acad. Sci. USA **87:**4164–4168.
14. **Freed, E. O., and M. A. Martin.** 1996. Domains of the human immunodeficiency virus type 1 matrix and gp41 cytoplasmic tail required for envelope incorporation into virions. J. Virol. **70:**341–351.
15. **Gibbs, J. S., D. A. Regier, and R. C. Desrosiers.** 1994. Construction and in vitro properties of HIV-1 mutants with deletions in nonessential genes. AIDS Res. Hum. Retroviruses **10:**343–350.
16. **Huang, Y., A. Khorchid, J. Gabor, J. Wang, X. Li, J.-L. Darlix, M. A. Wainberg, and L. Kleiman.** 1998. The role of nucleocapsid and U5 stem/A-rich loop sequences in $tRNA_3^{Lys}$ genomic placement and initiation of reverse transcription in human immunodeficiency virus type 1. J. Virol. **72:**3907–3915.
17. **Isel, C., C. Ehresmann, G. Keith, B. Ehresmann, and R. Marquet.** 1995. Initiation of reverse transcription of HIV-1: secondary structure of the HIV-1 RNA/$tRNA_3^{Lys}$ (template/primer) complex. J. Mol. Biol. **247:**236–250.
18. **Isel, C., R. Marquet, G. Keith, C. Ehresmann, and B. Ehresmann.** 1993. Modified nucleotides of tRNALys3 modulate primer/template loop-loop interaction in the initiation complex of HIV-1 reverse transcription. J. Biol. Chem. **268:**25269–25272.
19. **Kang, S.-M., and C. D. Morrow.** 1999. Genetic analysis of a unique human immunodeficiency virus type 1 (HIV-1) with a primer binding site complementary to $tRNA^{Met}$ supports a role for U5-PBS stem-loop RNA structures in initiation of reverse transcription. J. Virol. **73:**1818–1827.
20. **Lee, Y. M. H., and J. M. Coffin.** 1990. Efficient autointegration of avian retrovirus DNA in vitro. J. Virol. **64:**5958–5965.
21. **Masuda, T., M. J. Kuroda, and S. Harada.** 1998. Specific and independent recognition of U3 and U5 *att* sites by human immunodeficiency virus type 1 integrase in vivo. J. Virol. **72:**8396–8402.
22. **McBride, M. S., M. D. Schwartz, and A. T. Panganiban.** 1997. Efficient encapsidation of human immunodeficiency virus type 1 vectors and further characterization of *cis* elements required for encapsidation. J. Virol. **71:**4544–4554.
23. **Mizuuchi, K.** 1992. Transpositional recombination: mechanistic insights from studies of Mu and other elements. Annu. Rev. Biochem. **61:**1011–1051.
24. **Murphy, J. E., and S. P. Goff.** 1989. Construction and analysis of deletion mutations in the U5 region of Moloney murine leukemia virus: effects on RNA packaging and reverse transcription. J. Virol. **63:**319–327.
25. **Murphy, J. E., T. De Los Santos, and S. P. Goff.** 1993. Mutational analysis of the sequences at the termini of the Moloney murine leukemia virus DNA required for integration. Virology **195:**432–440.
26. **Pear, W. S., G. P. Nolan, M. L. Scott, and D. Baltimore.** 1993. Production of high-titer helper-free retroviruses by transient transfection. Proc. Natl. Acad. Sci. USA **90:**8392–8396.
27. **Pruss, D., F. D. Bushman, and A. P. Wolffe.** 1994. Human immunodeficiency virus integrase directs integration to sites of severe DNA distortion within the nucleosome core. Proc. Natl. Acad. Sci. USA **91:**5913–5917.
28. **Ratner, L., W. Haseltine, R. Patarca, K. L. Livac, B. Starcich, S. J. Josephs, E. R. Doran, J. A. Rafalski, E. A. Whitehorn, K. Baumeister, L. Ivanoff, R. R. Petteway, Jr., M. L. Pearson, J. A. Lauteenberger, T. S. Papas, J. Ghrayeb, N. T. Chang, R. C. Gallo, and F. Wong-Staal.** 1985. Complete nucleotide sequence of the AIDS virus, HTLV-III. Nature **313:**227–283.
29. **Ross, E. K., A. J. Buckler-White, A. B. Rabson, G. Englund, and M. A. Martin.** 1991. Contribution of NF-κB and Sp1 binding motifs to the replicative capacity of human immunodeficiency virus type 1: distinct patterns of viral growth are determined by T-cell types. J. Virol. **65:**4350–4358.
30. **Roth, M. J., P. L. Schwartzberg, and S. P. Goff.** 1989. Structure of the termini of DNA intermediates in the integration of retroviral DNA: dependence on IN function and terminal DNA sequence. Cell **58:**47–54.
31. **Salahuddin, S. Z., P. D. Markham, F. Wong-Staal, G. Franchini, V. S. Kalyanaraman, and R. C. Gallo.** 1983. Restricted expression of human T-cell leukemia-lymphoma virus (HTLV) in transformed human umbilical cord blood lymphocytes. Virology **129:**51–64.
32. **Salter, R. D., D. N. Howell, and P. Cresswell.** 1985. Genes regulating HLA class I antigen expression in T-B lymphoblast hybrids. Immunogenetics **21:**235–246.
33. **Sambrook, J., E. F. Fritsch, and T. Maniatis.** 1989. Molecular cloning: a laboratory manual, 2nd ed. Cold Spring Harbor Laboratory Press, Cold Spring Harbor, N.Y.

34. **Telesnitsky, A., and S. P. Goff.** 1997. Reverse transcriptase and the generation of retroviral DNA, p. 121–160. *In* J. M. Coffin, S. H. Hughes, and H. E. Varmus (ed.), Retroviruses. Cold Spring Harbor Laboratory Press, Cold Spring Harbor, N.Y.
35. **Wei, S.-Q., K. Mizuuchi, and R. Craigie.** 1997. A large nucleoprotein assembly at the ends of the viral DNA mediates retroviral DNA integration. EMBO J. **16:**7511–7520.
36. **Wei, S.-Q., K. Mizuuchi, and R. Craigie.** 1998. Footprints on the viral ends in Moloney murine leukemia virus preintegration complexes reflect a specific association with integrase. Proc. Natl. Acad. Sci. USA **95:**10535–10540.
37. **Weiss, A., R. L. Wiskocil, and J. D. Stobo.** 1984. The role of T3 surface molecules in the activation of human T cells: a two-stimulus requirement for IL 2 production reflects events occurring at a pretranslational level. J. Immunol. **133:**123–128.
38. **Zucker, M., and P. Stiegler.** 1981. Optimal computer folding of large RNA sequences using thermodynamics and auxiliary information. Nucleic Acids Res. **9:**133–148.